Since January 2020 Elsevier has created a COVID-19 resource centre with free information in English and Mandarin on the novel coronavirus COVID-19. The COVID-19 resource centre is hosted on Elsevier Connect, the company's public news and information website.

Science of the Total Environment 747 (2020) 141322

Contents lists available at ScienceDirect

Science of the Total Environment

journal homepage: www.elsevier.com/locate/scitotenv

Early spring near-surface ozone in Europe during the COVID-19 shutdown: Meteorological effects outweigh emission changes

Carlos Ordóñez [a,*], Jose M. Garrido-Perez [a,b], Ricardo García-Herrera [a,b]

[a] Dpto. Física de la Tierra y Astrofísica, Universidad Complutense de Madrid, Madrid, Spain
[b] Instituto de Geociencias (IGEO), CSIC-UCM, Madrid, Spain

HIGHLIGHTS

- Changes in NO_2 and O_3 have been assessed across Europe during the COVID-19 lockdown.
- The lockdown caused a substantial reduction in NO_2 concentrations across Europe.
- O_3 decreased in the Iberian Peninsula and increased in the rest of Europe.
- A considerable fraction of the O_3 changes can be explained by meteorological effects.
- Temperature, specific humidity and solar radiation were the most relevant variables.

GRAPHICAL ABSTRACT

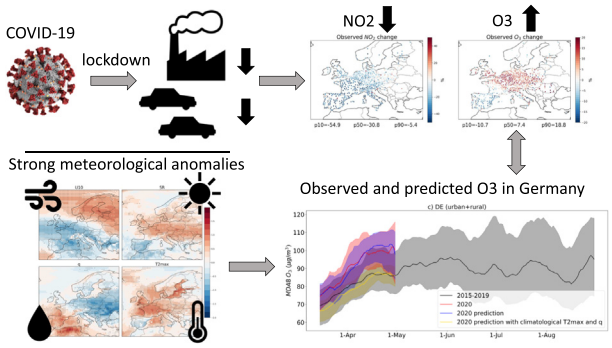

ARTICLE INFO

Article history:
Received 22 June 2020
Received in revised form 22 July 2020
Accepted 27 July 2020
Available online 28 July 2020

Keywords:
Air quality
Air pollution
Ozone
COVID-19
Coronavirus
NO_2

ABSTRACT

This paper analyses the impact of the control measures during the COVID-19 lockdown in Europe (15 March–30 April 2020) on 1-h daily maximum nitrogen dioxide (NO_2) and maximum daily 8-h running average ozone (MDA8 O_3) observations obtained from the European Environment Agency's air quality database (AirBase). Daily maximum NO_2 decreased consistently over the whole continent, with relative reductions ranging from 5% to 55% with respect to the same period in 2015–2019 for 80% of the sites considered (10th – 90th percentiles). However, MDA8 O_3 concentrations showed a different pattern, decreasing over Iberia and increasing elsewhere. In particular, a large region from northwestern to central Europe experienced increases of 10–22% at urban background stations, reaching typical values of the summer season. The analysis of the expected NO_2 and O_3 concentrations in the absence of the lockdown, using generalised additive models fed by reanalysis meteorological data, shows that the low NO_2 concentrations were mostly attributed to the emission reductions while O_3 anomalies were dominated by the meteorology. The relevance of each meteorological variable depends on the location. The positive O_3 anomalies in northwestern and central Europe were mostly associated with elevated temperatures, low specific humidity and enhanced solar radiation. This pattern could be an analogue to study the limits of pollution control policies under climate change scenarios. On the other hand, the O_3 reduction in Iberia is mostly attributable to the low solar radiation and high specific humidity, although the reduced zonal wind also played a role in the proximity of the Iberian Mediterranean coast.

1. Introduction

In December 2019, a novel virus named SARS-CoV-2 (severe acute respiratory syndrome coronavirus 2) causing COVID-19 (coronavirus

* Corresponding author.
E-mail address: carlordo@ucm.es (C. Ordóñez).

https://doi.org/10.1016/j.scitotenv.2020.141322
0048-9697/

disease 2019) was first reported in Wuhan, China. Since then, the virus has spread worldwide, leading the World Health Organization (WHO) to declare the COVID-19 outbreak a global pandemic on 11 March 2020 (Sohrabi et al., 2020). This airborne illness has not only caused an international health crisis, but also a great impact on society and the environment (Ivanov, 2020; Nicola et al., 2020; Yang et al., 2020). Most national governments have taken social distancing measures to reduce further spread and avoid the collapse of healthcare systems. As a consequence of the lockdown, unprecedented falls in industrial activity and vehicle use – two of the main sources of air pollution – have been reported. Consequently, the concentrations of several air pollutants have decreased in the affected countries (Bauwens et al., 2020; Chauhan and Singh, 2020; Petetin et al., 2020; Shi and Brasseur, 2020; Sicard et al., 2020; Tobías et al., 2020; Wang et al., 2020). As an illustration, Chauhan and Singh (2020) have documented the decline in particulate matter (PM) concentrations over some major cities around the world. Bauwens et al. (2020) have estimated a decrease in nitrogen dioxide (NO_2) tropospheric columns by 20–40% relative to the same period in 2019 over widespread areas of China, South Korea, western Europe and the United States. Wang et al. (2020) have linked the NO_2 reductions to the transportation sector in northern China, while the reduced emissions from the industrial sector were the main cause for the PM, carbon monoxide (CO) and sulphur dioxide (SO_2) decreases during the COVID-19 control period. Conversely, increases in near-surface ozone (O_3) have been reported. Shi and Brasseur (2020) have estimated an O_3 increase by a factor of 1.5–2 in northern China during winter. Sicard et al. (2020) also found O_3 enhancements in four southern European cities compared to the same spring period of the previous three years, with an average increase of 17%. Furthermore, O_3 concentrations increased in Rio de Janeiro during the lockdown because of the sharper decrease in nitrogen oxides ($NO_x \equiv NO+NO_2$) than in hydrocarbons (Siciliano et al., 2020).

Here we focus on the near-surface O_3 changes in Europe during the COVID-19 shutdown. This pollutant is produced in the troposphere by photochemical oxidation of non-methane volatile organic compounds (NMVOCs), CO and methane (CH_4), catalysed by NO_x and hydrogen oxide radicals (HO_x). Anthropogenic emissions are the main source of O_3 precursors, but the contribution of biogenic NMVOCs is also significant. Enhanced O_3 concentrations are usually associated with high temperatures and stagnant conditions, which favour photochemical production and the accumulation of O_3 (Jacob and Winner, 2009; Schnell and Prather, 2017; Sun et al., 2017; Garrido-Perez et al., 2019). The advection of polluted, warm air masses can also raise near-surface O_3 over some regions (Carro-Calvo et al., 2017; Garrido-Perez et al., 2019).

Elevated O_3 concentrations pose a serious threat to human health, the environment and climate. For instance, Cohen et al. (2017) estimated that exposure to ozone contributed to 254,000 (95% uncertainty interval 97,000–422,000) deaths globally in 2015. Ground-level ozone is also considered as the most detrimental air pollutant in terms of effects on vegetation (e.g. Mills et al., 2011). Furthermore, the past increase in tropospheric ozone is estimated to provide the third largest contribution to the rise in direct radiative forcing since the pre-industrial era (e.g. Unger et al., 2006). To reduce some of these impacts, the European Union has implemented air quality legislation over the last decades (Fowler et al., 2013; EU, 2016). Consequently, observational studies have shown a general decrease in the concentrations of ozone precursors over Europe (e.g. Georgoulias et al., 2019, for NO_2; Worden et al., 2013, for CO; Waked et al., 2016, and references therein, for NMVOCs). This does not necessarily have to result in reduced O_3 concentrations because the response of this pollutant to precursor emissions is non-linear. Overall, decreases in annual mean ozone concentrations have been reported at rural stations over the last years, associated with the reductions in NO_x and VOC emissions. On the other hand, ozone levels have risen at urban sites at least partly because of the reduced titration by nitrogen monoxide (NO) following the emission reductions. This has led to a convergence of ozone pollution for the different types of sites in Europe, although the concentrations remain higher at rural than at urban background sites (Sicard et al., 2013; Paoletti et al., 2014; Monks et al., 2015; Boleti et al., 2018).

While the enforcement of air pollution regulation is often aimed at gradual reductions of air pollutant concentrations, there have been specific events with stricter emission restrictions in the past, such as the 2008 Beijing Olympics (e.g. Wang et al., 2009; Witte et al., 2009). Nevertheless, the intensity, duration and extension of the decay in the emissions of primary pollutants during the COVID-19 lockdown are unprecedented, offering a unique opportunity to study the impact of reduced anthropogenic emissions on the O_3 concentrations at continental scales. On the other hand, the confounding effect of meteorological variability can complicate the attribution of changes in the pollutant concentrations to emission reductions. Petetin et al. (2020) have recently used machine learning algorithms to address this issue for NO_2 in Spain during the COVID-19 outbreak. Here we investigate the role played by meteorology in the observed changes of near-surface NO_2 and O_3 across Europe. For that purpose, we have used generalised additive models (GAMs) fed by reanalysis meteorological data to estimate the NO_2 and O_3 concentrations that would be expected in the absence of the lockdown.

2. Data and methods

2.1. Period of analysis and data sources

The response of European countries to the coronavirus outbreak has been diverse. The control measures to limit social contacts have been intensifying gradually under the criterion of each national government as the number of COVID-19 cases increased. The first measures were implemented around early March 2020 and most of the continent was under lockdown by mid-March. A few examples of the control measures are the suspension of crowd events, closure of education centres, shutdown of non-essential industrial and commercial activities, closure of international borders, internal border controls and restriction on people's movement. Once the health crisis stabilised, many countries started relaxing some of these measures in May 2020. Taking this sequence of events into account, we have chosen the period from 15 March to 30 April 2020 to evaluate the effects of these measures on air quality under the most exceptional conditions. For comparison purposes, the same time frame in 2015–2019 has been considered as a reference period.

We have used hourly NO_2 and O_3 concentrations during 2015–2020, extracted from the European Environment Agency's air quality database (AirBase) (https://www.eea.europa.eu/data-and-maps/data/aqereporting-8, last access: May 2020). At each station we calculate the daily maximum of the 1-h NO_2 averages and the maximum daily 8-h running average ozone (MDA8 O_3) for each day. The European Union uses these metrics to establish health based standards on the basis of epidemiological studies, with limit values of 200 μg/m^3 for hourly NO_2 and 120 μg/m^3 for MDA8 O_3 (https://ec.europa.eu/environment/air/quality/standards.htm, last access: June 2020). Only the stations catalogued as background with at least 75% of the data available during both the study and reference periods have been considered in this work. This way we have selected a total of 1331 sites (984 urban background and 347 rural) for NO_2 and 1376 (915 urban background and 461 rural) for O_3, while the traffic stations are not considered. Fig. S1 displays the spatial distribution of the monthly MDA8 O_3 means at those sites, illustrating that the March–April period investigated here can be considered as a transition time between the low ozone months (Oct–Feb) and the high ozone season (from April to September, depending on the region). The analyses presented in this work have first been performed separately for urban background and rural stations. Since both types of sites exhibit the same patterns, we will

show the results for the combination of them throughout the manuscript.

For the characterization of the meteorological conditions, we have extracted the following fields from the ERA5 meteorological reanalysis (Hersbach et al., 2020), at 0.75° × 0.75° horizontal resolution, for the 1981–2020 period: daily maximum air temperature at 2 m (T2max); daily mean fields of the zonal (U10) and meridional (V10) wind components at 10 m, 500 hPa geopotential height (Z500), 2-m specific humidity (q) and downward solar radiation flux (SR), and daily accumulated precipitation (Prec). Although ERA5 data may have some deficiencies in capturing the local meteorology at some sites, the resolution used here seems to be appropriate as shown by previous analyses on the influence of meteorology on surface ozone observations in Europe (Otero et al., 2016; Boleti et al., 2020). Furthermore, additional analyses based on NCEP/NCAR meteorological data at 2.5° × 2.5° (Kalnay et al., 1996) confirm that the results presented in this work are not very sensitive to the choice of the reanalysis dataset (not shown).

2.2. Statistical model

A generalised additive model (GAM) is a multivariate semi-parametric regression model that accounts for the additive effect of the predictors on the predictand and their non-linear relationships. This tool is commonly used to quantify the influence of meteorology on air pollutant time series (Dominici et al., 2002; Barmpadimos et al., 2011; Pearce et al., 2011; Boleti et al., 2018). We have applied this statistical technique, provided by the pyGAM Python module (Servén and Brummitt, 2018), to each site separately in order to characterise the relationship between the air pollutant concentrations and meteorological variables. We have built the models using March and April data from 2015 to 2019. In addition to the meteorological drivers mentioned in Section 2.1, we have also included the occurrence of working vs. non-working days in the models as it is known to affect the day-to-day evolution of air pollution. This is considered as a categorical variable that treats both the weekends and Easter holidays as non-working days. While the model uses spline functions to estimate the pollutant response to continuous variables, the categorical variables are fit using factor functions, with fixed constant values for each categorical attribute. The general form of the model used in this work is as follows:

$$Y = \beta_0 + \sum_x s_x(A_x) + \sum_y f_y(B_y) \quad (1)$$

where Y: pollutant concentration (1-h daily maximum NO_2 or MDA8 O_3). β_0: intercept of the model. $s_x(A_x)$: smoothing spline function on continuous feature A_x (meteorological field). $f_y(B_y)$: factor function on categorical feature B_y (working or non-working day).

The resulting deviance explained by the GAMs for March–April 2015–2019 is satisfactory for most locations, with the median across all sites ranging from 48% for NO_2 to 60% for O_3 (Fig. S2). The spatial distribution shows the best performance for NO_2 in Benelux (with values up to ~65%) and for O_3 in the inner part of the continent (~80%). In addition, the examination of residuals indicates normal distributions, with no significant biases and constant residual variance (homocedasticity), evidencing the consistency of the model (not shown).

3. Impact of emission changes and meteorology on O_3 during early spring 2020

The left panels of Figs. 1 and S3 illustrate the concentration anomalies (in % and μg/m^3, respectively) of NO_2 (top) and O_3 (bottom) at background sites during 15 March – 30 April 2020 with respect to the same period in 2015–2019. As expected, the emission reductions yielded decreases in the NO_2 concentrations at most sites. This is particularly

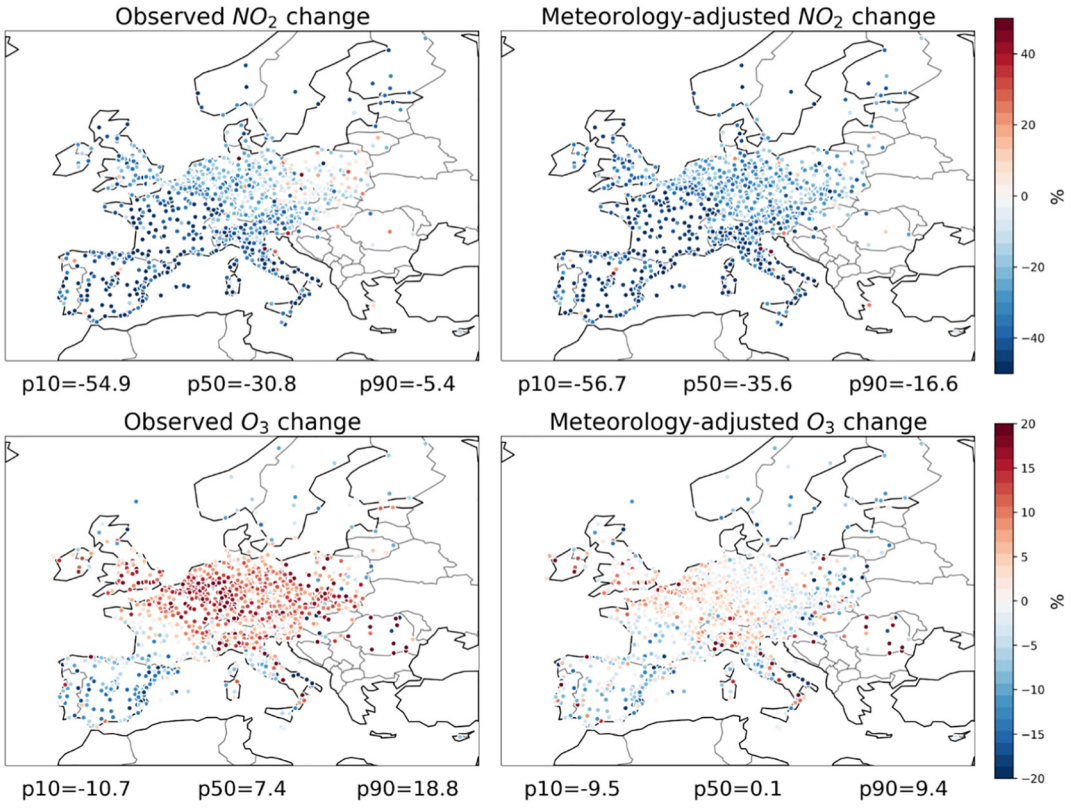

Fig. 1. Left panels: Average anomalies (%) of the observed 1-h daily maximum NO_2 (top) and MDA8 O_3 (bottom) concentrations at background sites during 15 March – 30 April 2020 with respect to those of the same period in 2015–2019. Right: Average meteorologically-adjusted changes (%) of the same pollutants during 15 March – 30 April 2020, calculated as the difference between the observed concentrations and the concentrations estimated by the GAMs described in Section 2.2. The numbers below the panels respectively indicate the 10th, 50th and 90th percentiles (p10, p50, p90) across all sites. The corresponding absolute values (μg/m^3) can be found in Fig. S3.

Table 1
Left: Average anomalies ± standard deviation (%) of the observed 1-h daily maximum NO_2 and MDA8 O_3 concentrations during 15 March – 30 April 2020 with respect to those of the same period in 2015–2019, summarised by country and site type. Right: Average meteorologically-adjusted changes ± standard deviation (%) of the same pollutants during 15 March – 30 April 2020, calculated as the difference between the observed concentrations and the concentrations estimated by the GAMs described in Section 2.2, summarised by country and site type.

	Observed changes (%)				Meteorology-adjusted changes (%)			
	NO_2		O_3		NO_2		O_3	
	Urban	Rural	Urban	Rural	Urban	Rural	Urban	Rural
Austria	−25.1 ± 8.3	−23.0 ± 9.4	11.7 ± 6.0	5.6 ± 5.5	−34.4 ± 5.9	−27.6 ± 9.2	0.5 ± 5.6	−3.3 ± 4.3
Belgium	−30.2 ± 7.1	−26.8 ± 12.2	22.2 ± 8.5	14.0 ± 3.5	−36.3 ± 7.2	−35.7 ± 10.3	8.7 ± 6.7	3.2 ± 3.4
Czech Republic	−3.7 ± 8.3	−15.2 ± 21.8	10.8 ± 6.4	9.8 ± 2.7	−18.8 ± 6.0	−22.8 ± 17.9	−2.0 ± 5.3	−2.5 ± 2.7
Germany	−16.0 ± 9.2	−21.4 ± 16.0	14.5 ± 5.4	9.4 ± 5.1	−25.9 ± 7.6	−26.0 ± 13.0	2.5 ± 4.1	−0.3 ± 3.6
Spain	−51.6 ± 11.2	−38.4 ± 27.9	−7.1 ± 10.7	−11.6 ± 6.9	−50.0 ± 11.9	−39.4 ± 26.6	−1.7 ± 11.6	−7.8 ± 7.3
France	−43.1 ± 11.4	−36.7 ± 19.6	6.6 ± 9.6	3.1 ± 7.7	−46.9 ± 9.8	−42.3 ± 17.0	1.7 ± 6.8	−2.1 ± 5.0
United Kingdom	−31.2 ± 12.9	−21.5 ± 12.7	12.3 ± 13.9	3.1 ± 6.7	−35.0 ± 11.9	−31.7 ± 11.0	4.7 ± 11.4	−1.2 ± 5.5
Italy	−44.2 ± 13.9	−25.7 ± 25.8	5.0 ± 13.1	1.2 ± 16.0	−48.4 ± 13.7	−32.2 ± 26.3	1.9 ± 12.2	−2.2 ± 14.7
Netherlands	−26.4 ± 5.4	−19.1 ± 10.8	14.1 ± 5.8	12.2 ± 4.3	−27.0 ± 4.5	−22.3 ± 11.1	3.8 ± 4.6	3.4 ± 5.0
Poland	−5.3 ± 16.9	−12.1 ± 15.1	10.5 ± 9.5	3.8 ± 11.1	−23.7 ± 12.9	−18.7 ± 18.2	−3.5 ± 8.8	−7.2 ± 9.3

noticeable for Spain, France and Italy, where some of the strictest lockdown measures were implemented. The few locations with positive anomalies are mainly restricted to Poland and the surrounding countries. On the other hand, O_3 concentrations increased over most of Europe, except for the Iberian Peninsula, southern and western France, central Italy and some locations of northern Europe (e.g. in Scotland and Scandinavia).

As the lockdown measures were not implemented uniformly and simultaneously across the European states, we have quantified the changes in the NO_2 and O_3 concentrations separately for each country (Table 1 left). To draw solid conclusions, this has been done only for those countries with good coverage of urban background and rural measurement sites (>25 stations for both NO_2 and O_3). The table confirms the strongest NO_2 decreases found for the three mentioned countries (Spain, France and Italy), with a fall of more than 40% from the baseline for urban background stations. This order of magnitude is comparable to that of the ~50% NO_2 reductions (ranging from 30% to 69%) reported by Sicard et al. (2020) and Tobías et al. (2020) for five cities in the same countries. Conversely, averaged O_3 concentrations increased both at urban background and rural sites in all countries except for Spain. This needs to be further investigated, bearing in mind that ozone concentrations do not respond linearly to changes in precursor emissions (e.g. Lin et al., 1988; Trainer et al., 1993; Parrish et al., 1999; Vogel et al., 1999; Sillman, 1999; Kleinman et al., 2002). The fact that O_3 increased more at urban than at rural sites in 9 of the 10 countries considered (and decreased less at urban than at rural sites in Spain) indicates the diminished effect of titration by NO at the urban sites following the reduction in anthropogenic emissions (e.g. Ordóñez et al., 2005; Tonse et al., 2008; Monks et al., 2015; Sicard et al., 2020; Tobías et al., 2020). Nevertheless, the decreases and the smallest increases in O_3 at

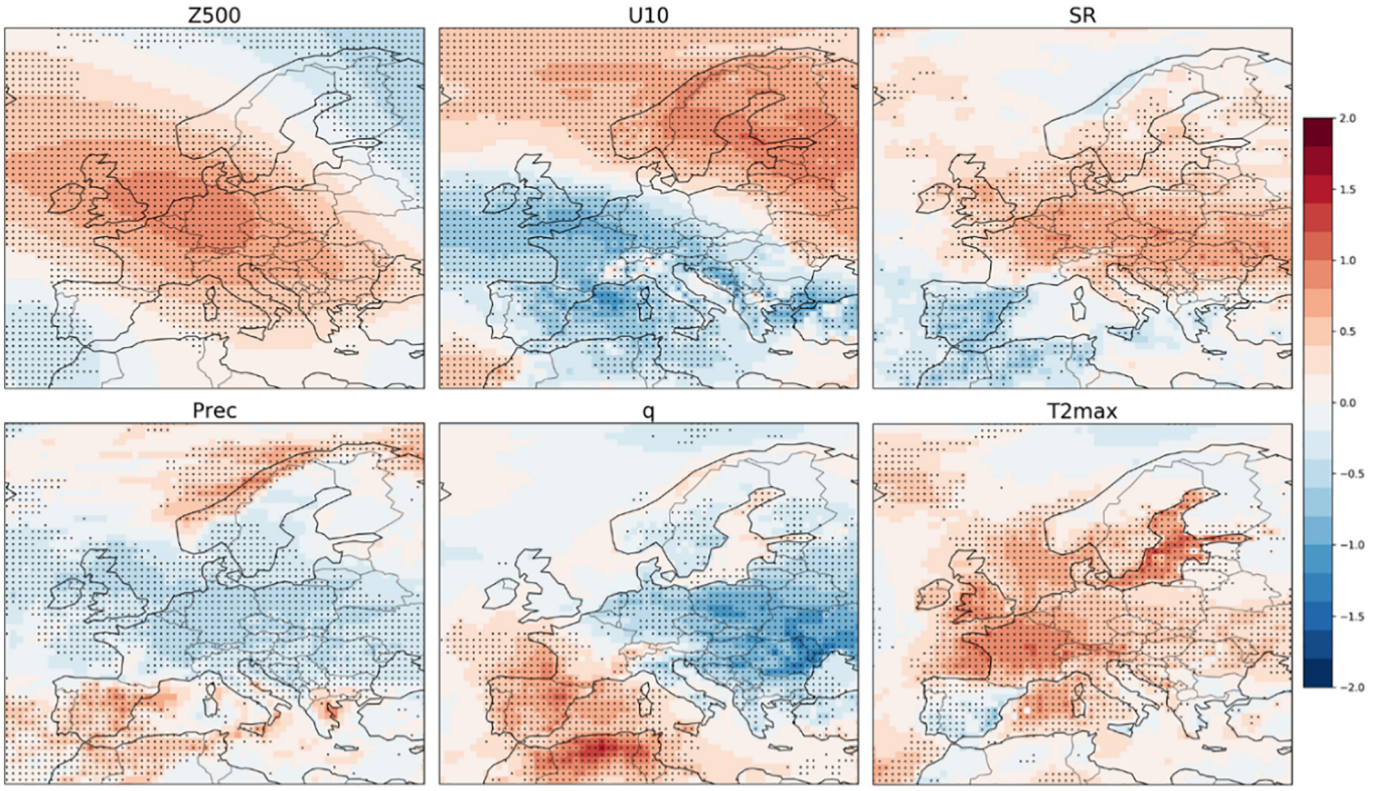

Fig. 2. Standardised anomalies of meteorological fields (Z500, 10-m zonal wind, incoming solar radiation flux at surface, precipitation, 2-m specific humidity, 2-m daily maximum temperature) during 15 March – 30 April 2020 with respect to the same period in 1981–2010. Stippling indicates grid cells where the 2020 and 1981–2010 distributions are statistically different at the 95% confidence level (determined through two-sample Kolmogorov-Smirnov tests).

the two types of sites were found for the three countries with the strongest NO_2 reductions (Spain, France and Italy). On the other hand, significant ozone production downwind of the sources only occurs under periods of sustained sunshine and relatively high temperatures. Therefore, the role of the meteorology needs to be examined too.

To assess whether the meteorological conditions in early spring 2020 resembled those of an average year, we have computed the standardised anomalies of some meteorological fields during 15 March – 30 April 2020 with respect to the same period in 1981–2010 (Fig. 2). Significantly positive Z500 anomalies occurred over large parts of Europe (apart from the southwest and northeast of the domain), resulting in supressed zonal winds in the lower levels. Overall, there was a strong contrast between the Iberian Peninsula and the rest of Europe. The former region, with significantly positive anomalies of precipitation and specific humidity as well as significantly negative anomalies of solar radiation and temperature, was the only region of western Europe where weather conditions were more adverse than average to ozone production. The opposite holds true for the rest of western and central Europe. As Iberia is the only region where O_3 concentrations in 2020 were lower than in the 2015–2019 reference period, these results suggest that weather conditions inhibited ozone production there, highlighting the need for disentangling the impacts of meteorology and emission changes.

To remove the effect of meteorology on air quality during early spring 2020, we have first estimated the NO_2 and O_3 concentrations that would be expected at each location from the meteorology of that year in the absence of the stringent lockdown measures taken in Europe. For that purpose, we have applied the GAMs described in Section 2.2, trained with 2015–2019 meteorology, considering the weather conditions of each day in early spring 2020. The difference between the observed and the predicted concentrations can be considered as the meteorologically adjusted NO_2 and O_3 changes in 2020. These are shown in the right panels of Figs. 1 and S3. The spatial distribution of meteorologically adjusted NO_2 changes resembles that of observed NO_2 (top left panel), but with slightly larger negative anomalies. The largest differences are located over central Europe due to the adverse effects of meteorology in 2020, which partly compensate the NO_2 reduction. The same results are found when the NO_2 changes in 2020 are examined for groups of stations and countries (Table 1). This indicates the strong impact of the lockdown measures on the NO_2 concentrations across Europe, with a moderate impact of the meteorological conditions for most sites. On the other hand, when the effect of the meteorology is removed, the spatial patterns of the ozone changes (lower right panel of Fig. 1) are less marked than those observed (lower left panel). Both the magnitude of the anomalies and the number of sites with positive anomalies decrease considerably, resulting in small ozone decreases when averaged over the rural sites for most countries (Table 1). These results suggest that only part of the O_3 enhancements observed during 2020 compared with previous years (Fig. 1, bottom left) can be ascribed to the reduction in ozone precursor emissions (Fig. 1, bottom right), and that the stable/unsettled weather conditions in central Europe/Iberia also played a role.

We have devised a portioning approach to identify the main components (from the fields used to feed the GAMs) responsible for the meteorologically driven ozone changes in 2020 with respect to 2015–2019. For each meteorological field, we have replaced its daily values during 15 March – 30 April 2020 by the climatological values (15-day moving averages around each calendar day in 2015–2019) to recalculate the O_3 concentrations in 2020. The contribution of a given component to the meteorologically driven O_3 changes is defined as the difference between the O_3 concentrations predicted by a model with daily meteorological fields in 2020 and an analogous model where the climatological values are used for that component. The contributions of some of the most relevant fields to the ozone changes with respect to 2015–2019 are shown in Fig. 3 (top panels), which can be compared with the meteorological anomalies of Fig. 2. First, the high (low) solar radiation in 2020 yielded moderate ozone increases (decreases) over most of Europe (Iberia). These changes are relatively small (from around −2 to 4 $\mu g\ m^{-3}$, excluding the lowest and highest deciles), most probably because the effects of radiation are offset by the influence of other fields such as temperature and specific humidity. In fact, elevated temperatures drove O_3 increases of 6–9 $\mu g\ m^{-3}$ at many sites of western and central Europe (around half of the observed changes, see Fig. S3) as well as moderate decreases in the south of the continent. The positive specific humidity anomalies in Iberia as well as in western and southern France are consistent with the O_3 decreases driven by this field in those regions (exceeding 4 $\mu g\ m^{-3}$ at some sites in Iberia). On the other hand, the negative humidity anomalies in the centre of the continent yielded O_3 increases of similar magnitude, although with the location of the maximum values clearly shifted to the east, compared to those due to temperature. Finally, the reduced zonal flow in the lower levels is associated with rises in the O_3 concentrations up to ~3 $\mu g\ m^{-3}$ (90th percentile) at many sites of Europe, with the main exception of some areas in France, Switzerland and the neighbouring regions. Note that one should not always expect a good correspondence between the meteorological anomalies and the ozone changes potentially driven by those fields for the following reasons. First, the reference periods considered here are different (1981–2010 climatology for meteorology in Fig. 2 and 2015–2019 for ozone in Fig. 3). Second, GAMs consider non-linear relationships between ozone and the meteorology. Finally, there is some co-linearity between the meteorological fields, which could offset some potential relationships as mentioned for solar radiation. Nevertheless, most of the relationships found here are in line with the well-known mechanisms that explain the association between O_3 and meteorology.

The main component of the meteorologically driven O_3 changes at each location in 2020 has been identified as that yielding the highest O_3 change between both models. The spatial patterns of Fig. 3 (bottom panel) confirm the major impact of high temperatures on the ozone enhancements over the British Isles, France, Benelux and Germany. Similar results apply to the reduced specific humidity in Eastern Europe, while the enhanced solar radiation is the most relevant meteorological driver at some clusters of sites around northern Italy and Austria. In Iberia, the low solar radiation and high specific humidity controlled the modelled O_3 decreases with respect to the reference period, whereas the reduced zonal flow also played a fundamental role in the proximity of the Mediterranean coast.

4. Regional analysis for central and southwestern Europe

Here we conduct more in-depth analyses for Spain and Germany as representative countries with opposite sign in the observed O_3 concentration anomalies. As the ozone concentrations were particularly high for that time of the year in Germany and the surrounding countries, we also compare them with the spring-summer climatology of the previous years. This way we can determine whether the observed anomalies in early spring 2020 were within the range of expectations or if the concentrations were close to those of the typical summer ozone season.

Fig. 4 illustrates the time series of the 15-day moving average NO_2 and O_3 concentrations in Germany and Spain during 15 March – 31 August of the 2015–2019 reference period. The black lines represent the median concentrations across all sites and years, while the grey shading encompasses the body of data between the 25th and 75th percentiles. We have also plotted the observed concentrations (red) and the concentrations predicted by the GAMs (blue) for 15 March – 30 April 2020. The observed NO_2 concentrations (panels a and b, red colours) are clearly below the reference values (grey) for all percentile ranges in both countries because of the COVID-19 shutdown. When we predict the NO_2 concentrations with the meteorology of 2020 (blue) they become close to the reference in the case of Iberia and somewhat higher for Germany, most probably because of the stagnant conditions over central Europe during 2020. As documented above, the observed

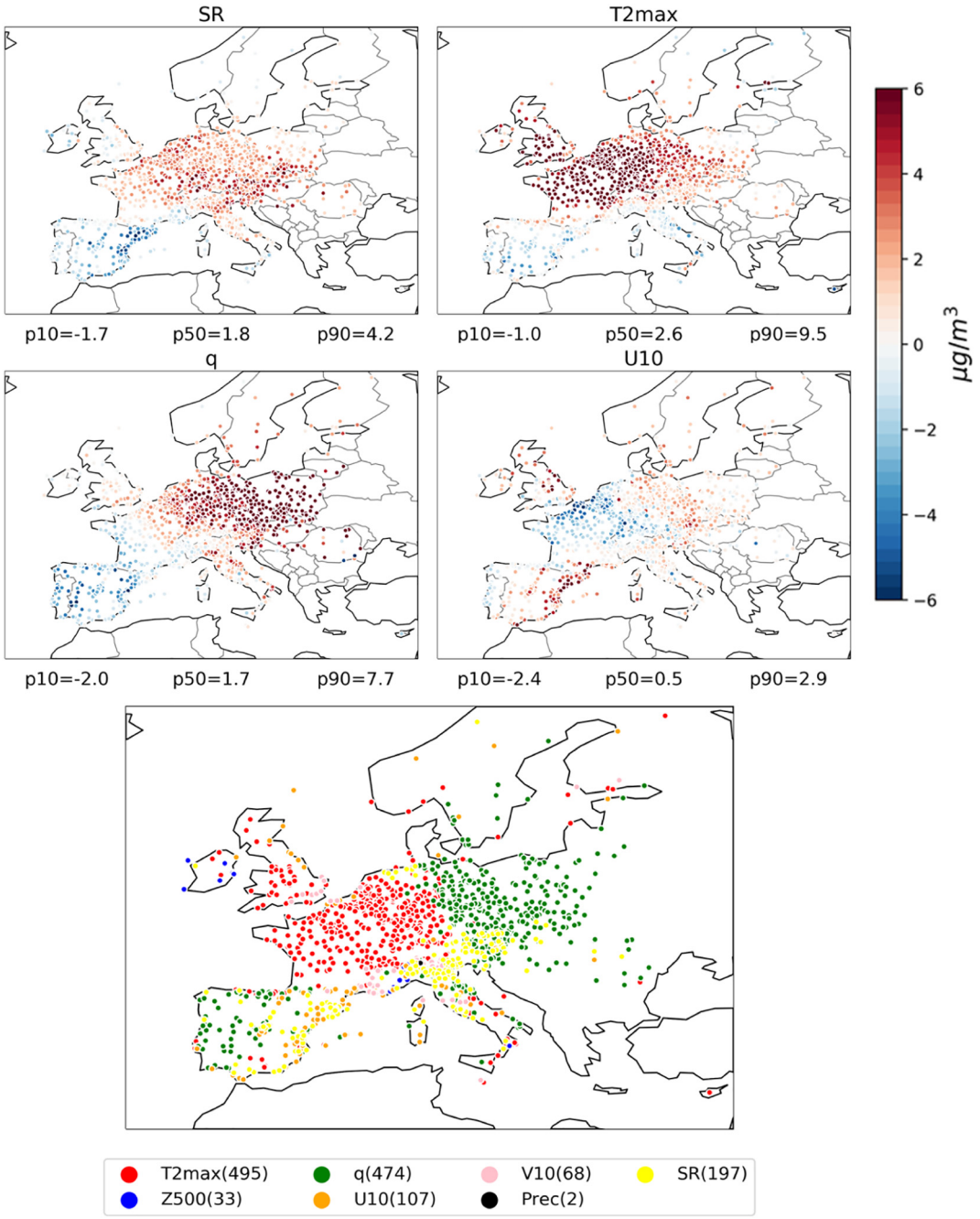

Fig. 3. Top panels: Average differences between predicted MDA8 O_3 at background sites using daily meteorology of 15 March – 30 April 2020 and after replacing the daily values of a meteorological field (from left to right and from top to bottom: incoming solar radiation at surface, 2-m daily maximum temperature, 2-m specific humidity, 10-m zonal wind) by the climatological values (15-day running means around each calendar day in 2015–2019). Bottom panel: Map displaying the dominant meteorological component of the MDA8 O_3 anomalies. The number of sites for each meteorological component is indicated in brackets.

ozone concentrations (panels c and d, red colours) were above/below the reference concentrations (grey) for Germany/Spain. In the latter country, the observed ozone medians were closer to the 25th percentiles than to the climatological medians most of the time, while the values predicted by the model (blue) were still low but somewhat closer to the climatological values. Again, this indicates that the combination of low emissions and unsettled weather contributed to the low ozone concentrations in Spain. If daily downward solar radiation fluxes and specific humidity in 2020 are replaced by their reference values (15-day moving averages around each calendar day during 2015–2019), the concentrations predicted by the GAMs (golden) become closer to the reference ones, confirming that below average solar radiation and above average humidity contributed to the low ozone concentrations in southwestern Europe during that year (Fig. 3).

The observed ozone concentrations in Germany during spring 2020 are considerably higher than the reference ones (Fig. 4c). The rise from March to April is steeper than in the reference climatology, resulting in median values during the last weeks of April well above the summer medians of the reference period. This is remarkable because, despite the moderate seasonality of ozone during spring and summer in Germany, the peak ozone season over most of the country occurs between June and August (see also Fig. S1). On the other hand, the 75th percentiles in April 2020 do not differ much from those of June–August of the reference period. This probably occurs partly because

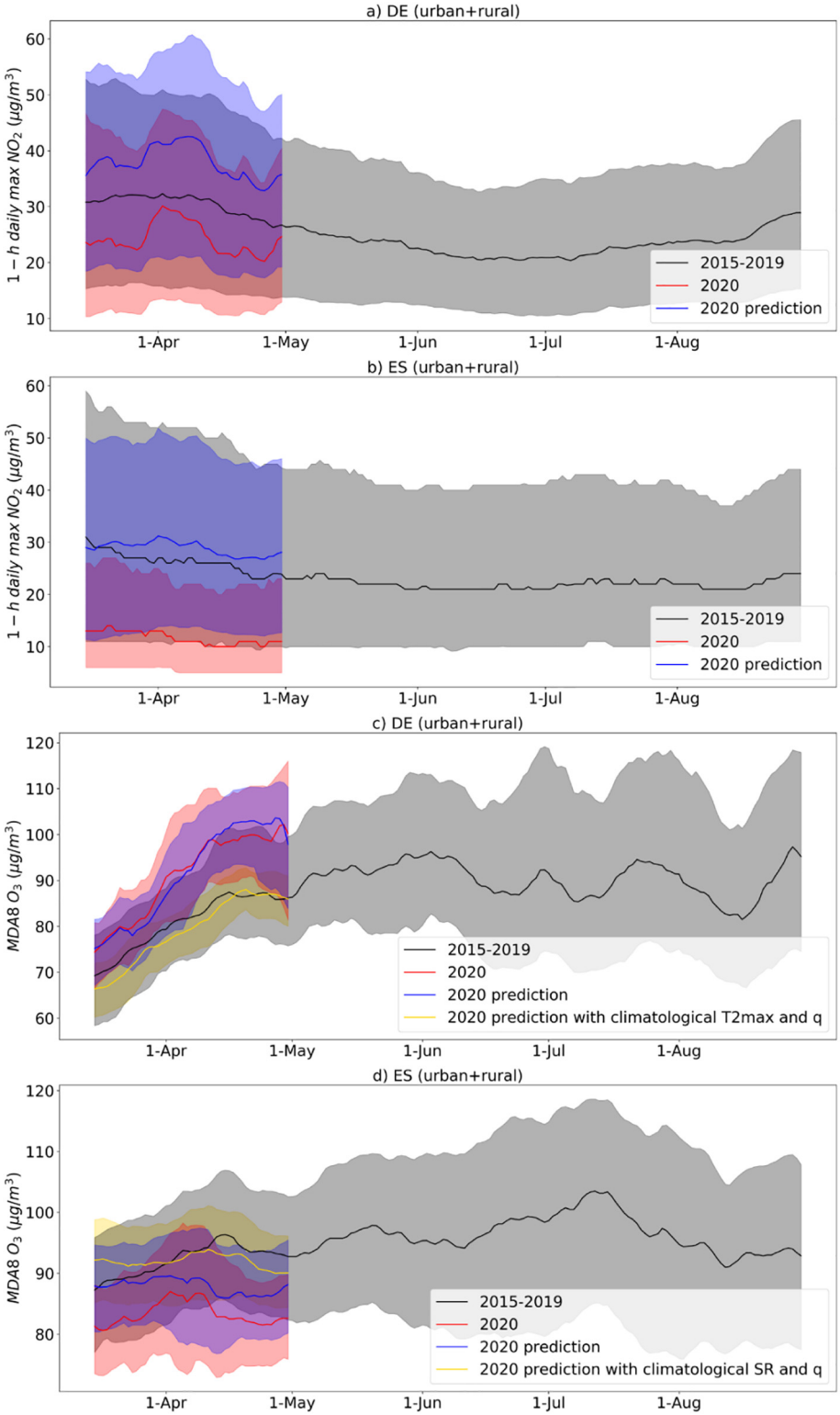

Fig. 4. Time series of the 15-day moving averages of 1-h daily maximum NO_2 (a, b) and MDA8 O_3 (c, d) concentrations at background sites in Germany and Spain. The time series included here correspond to observations during the reference period 15 March – 31 August 2015–2019 (grey), observations during 15 March – 30 April 2020 (red), GAM predictions using daily meteorology of that period (blue) and GAM predictions for the same period after replacing some meteorological fields (daily maximum temperature and specific humidity for Germany, solar radiation and specific humidity for Spain) by 15-day moving averages around each calendar day of 2015–2019 (golden). Solid lines depict the medians across all sites and shading indicates the range between the 25th and 75th percentiles.

the distribution gets narrower when only one year of data is considered, although it is also known that the middle and high ozone percentiles often respond differently to emissions and meteorological changes (e.g. Ordóñez et al., 2005; Paoletti et al., 2014; Yan et al., 2018). If we predict the ozone concentrations in Germany with the meteorology of 2020 (blue), they remain high compared to the April climatology, indicating that the meteorological conditions during the COVID-19 shutdown favoured ozone production. When daily maximum temperature

and specific humidity are replaced by those of the reference period (gold), the predicted ozone concentrations decrease by up to ~15 μg m^{-3} and get close to the climatology towards the end of April, confirming the predominant role of elevated temperatures and low humidity in raising the ozone concentrations to the typical summer levels.

Summarising, the results for both countries indicate that (i) the emission reductions explain the low NO_2 concentrations observed during 15 March – 30 April 2020, (ii) both meteorology and emission reductions contributed to the low ozone concentrations measured in Spain, and (iii) meteorological effects were responsible for the high ozone concentrations in Germany. Our conclusions remain the same when urban background and rural sites are treated separately (not shown).

On the other hand, there are some regions (e.g. southern England, the northern coast of France, Benelux and northern Italy) as well as some isolated locations where considerable ozone increases are still found for the same period after the meteorological adjustment (lower right panels of Figs. 1 and S3). It is not particularly striking to find ozone enhancements under reduced NO_x concentrations. This has previously been found for different locations of the globe due to the high nonlinearity in NO_x-VOC-HO_x chemistry (e.g. Thielmann et al., 2001; Jhun et al., 2015; Saiz-Lopez et al., 2017; Li et al., 2019). This is more likely to occur outside the warm season and in polluted areas, where NO_x decreases reduce the ozone loss by titration (e.g. Sillman, 1999; Ordóñez et al., 2005; Jonson et al., 2006; Jhun et al., 2015). It might well be that many observational sites in Europe – with 24-h mean NO_2 concentrations around 20 μg m^{-3} and 8 μg m^{-3} when averaged over all urban background and rural sites, respectively, during the 2015–2019 reference period – are often in the high NO_x regime at this time of the year, which would imply higher ozone concentrations under reduced NO_x emissions. Moreover, with the traffic restrictions, the concentrations of NO_x might have decreased more than those of NMVOCs in some parts of Europe, leading to enhanced NMVOC/NO_x ratios and amplified ozone pollution, as suggested by Sicard et al. (2020) for some southern European cities and proved by Siciliano et al. (2020) for Rio de Janeiro. In addition, reduced aerosol loadings during the prolonged shutdown could also lead to ozone enhancements through increased photolysis rates (e.g. Hollaway et al., 2019) and diminished uptake of hydroperoxyl radicals (HO_2) that remove NO from the atmosphere (Li et al., 2019).

Despite the unquestionable impact of the meteorology found by our analyses, regional chemistry modelling or idealised photochemical box modelling studies of this episode are needed to understand the reasons for the different behaviour in Iberia and other regions of Europe. A recent chemical transport model study of the lockdown effects on atmospheric composition in Europe during March 2020 points to higher ozone increases (or lower ozone decreases) at urban than at rural sites (Menut et al., 2020), as found here for meteorologically adjusted ozone changes (Table 1), although more dedicated analyses are needed due to the existence of non-linear chemical effects. Simultaneous observations of precursors, ozone and other oxidants, if available, may be of great value to understand these differences, as recently done by Siciliano et al. (2020) for Rio de Janeiro.

5. Summary and conclusions

As a result of the COVID-19 pandemic, strict lockdown measures were implemented by most European governments from 15 March to 30 April 2020, with unprecedented travel restrictions and reduction in non-essential business and industrial activities. Consequently, the atmospheric concentrations of NO_2 decreased across Europe in comparison with the same period during the reference years 2015–2019. Among the ~1300 background stations considered in this work, 80% of the sites (10th – 90th percentiles) show decreases in 1-h daily maximum NO_2 ranging from 5% to 55%, with the highest reductions located in Spain, France and Italy (>40% on average at urban background sites). Ozone concentrations presented a different pattern, with decreases over Iberia and increases elsewhere. While urban MDA8 O_3 was on average around 7% lower than in the reference period for Spain, it increased in a range between 5% and 22% for the rest the countries considered in this work, reaching values comparable to those of a typical summer over some regions.

We have identified strong meteorological anomalies, with conditions favourable for the accumulation of primary pollutants and ozone production over large parts of Europe and unsettled weather in the southwest of the continent. To investigate whether the contrasting weather conditions can explain some of the regional differences in ozone, we have built statistical models that account for the observed dependence of the NO_2 and O_3 concentrations on the meteorology. With this we have estimated the concentrations that could be expected with the meteorology of March–April 2020 in the absence of the lockdown. The following conclusions can be drawn from these analyses:

- The low NO_2 concentrations are mostly attributed to the emission reductions. The stable weather conditions, with reduced ventilation and precipitation over large parts of Europe, could not offset the emission reductions. The meteorologically adjusted NO_2 decreases are larger than observed due to these meteorological conditions, especially in central and Eastern Europe.
- Meteorological effects contributed to lowering ozone concentrations in Iberia and raising them in the rest of Europe, explaining a large proportion of the observed changes.
- The main meteorological variables driving the ozone anomalies vary with the geographical location. They were dominated by elevated temperatures in the British Isles, France, Benelux and Germany (leading up to a ~9–10 μg m^{-3} increase in the period-average MDA8 O_3); low specific humidity in Eastern Europe (~7–8 μg m^{-3} increase); elevated solar radiation around northern Italy and Austria (~3–4 μg m^{-3} increase), and low solar radiation, high specific humidity and reduced zonal wind in the Iberian Peninsula.

The restrictions to people's mobility and fall in economic activity during the COVID-19 lockdown offer a unique opportunity to test the efficiency of strict emission controls in reducing ground-level ozone. Our results point to a dominant role of meteorology on the regional ozone anomalies in Europe during the lockdown period as well as to differing ozone responses to emission changes. Future modelling studies, complemented by observational studies if arrays of simultaneous observations of ozone and precursors are available at some locations, are needed to understand changes in the oxidation capacity of the atmosphere and the potential existence of different chemical regimes leading to divergent regional ozone responses under such strict emission reductions. These results can also be useful to study the limits of pollution abatement policies in climate change scenarios, since the meteorological conditions over large parts of Europe during the period of analysis can be considered as analogous of the projected warming for the region throughout the 21st century (Christensen et al., 2013).

CRediT authorship contribution statement

Carlos Ordóñez: Conceptualization, Methodology, Writing - original draft, Funding acquisition. **Jose M. Garrido-Perez:** Conceptualization, Methodology, Software, Formal analysis, Writing - review & editing. **Ricardo García-Herrera:** Conceptualization, Methodology, Writing - review & editing.

Declaration of competing interest

The authors declare that they have no known competing financial interests or personal relationships that could have appeared to influence the work reported in this paper.

Acknowledgements

This work was supported by the Spanish Ministerio de Economía y Competitividad [grant number RYC-2014-15036] and the Spanish Ministerio de Educación, Cultura y Deporte [grant number FPU16/01972]. We also acknowledge support from STEADY (CGL2017-83198-R), project funded by the Spanish Ministerio de Economía, Industria y Competitividad. The authors are grateful to the European Environment Agency for making NO_2 and O_3 data available through the Air-Base air quality database as well as to NOAA/OAR/ESRL PSD for providing NCEP reanalysis data. The authors thank the anonymous reviewers and editors for their constructive and useful comments.

Appendix A. Supplementary data

Supplementary data to this article can be found online at https://doi.org/10.1016/j.scitotenv.2020.141322.

References

Barmpadimos, I., Hueglin, C., Keller, J., Henne, S., Prévôt, A.S.H., 2011. Influence of meteorology on PM_{10} trends and variability in Switzerland from 1991 to 2008. Atmos. Chem. Phys. 11, 1813–1835. https://doi.org/10.5194/acp-11-1813-2011.

Bauwens, M., Compernolle, S., Stavrakou, T., Müller, J.-F., Gent, J., Eskes, H., Levelt, P.F., A, R., Veefkind, J.P., Vlietinck, J., Yu, H., Zehner, C., 2020. Impact of coronavirus outbreak on NO_2 pollution assessed using TROPOMI and OMI observations. Geophys. Res. Lett. 47, 1–9. https://doi.org/10.1029/2020gl087978.

Boleti, E., Hueglin, C., Takahama, S., 2018. Ozone time scale decomposition and trend assessment from surface observations in Switzerland. Atmos. Environ. 191, 440–451. https://doi.org/10.1016/j.atmosenv.2018.07.039.

Boleti, E., Hueglin, C., Grange, S.K., Prévôt, A.S.H., Takahama, S., 2020. Temporal and spatial analysis of ozone concentrations in Europe based on timescale decomposition and a multi-clustering approach. Atmos. Chem. Phys. 20, 9051–9066. https://doi.org/10.5194/acp-20-9051-2020.

Carro-Calvo, L., Ordóñez, C., García-Herrera, R., Schnell, J.L., 2017. Spatial clustering and meteorological drivers of summer ozone in Europe. Atmos. Environ. 167, 496–510. https://doi.org/10.1016/j.atmosenv.2017.08.050.

Chauhan, A., Singh, R.P., 2020. Decline in $PM_{2.5}$ concentrations over major cities around the world associated with COVID-19. Environ. Res. 187, 109634. https://doi.org/10.1016/j.envres.2020.109634.

Christensen, J.H., Krishna Kumar, K., Aldrian, E., An, S.-I., Cavalcanti, I.F.A., de Castro, M., Dong, W., Goswami, P., Hall, A., Kanyanga, J.K., Kitoh, A., Kossin, J., Lau, N.-C., Renwick, J., Stephenson, D.B., Xie, S.-P., Zhou, T., 2013. Climate phenomena and their relevance for future regional climate change. In: Stocker, T.F., Qin, D., Plattner, G.-K., Tignor, M., Allen, S.K., Boschung, J., Nauels, A., Xia, Y., Bex, V., Midgley, P.M. (Eds.), Climate Change 2013: The Physical Science Basis. Contribution of Working Group I to the Fifth Assessment Report of the Intergovernmental Panel on Climate Change. Cambridge University Press, Cambridge, United Kingdom and New York, NY, USA.

Cohen, A.J., Brauer, M., Burnett, R., Anderson, H.R., Frostad, J., Estep, K., Balakrishnan, K., Brunekreef, B., Dandona, L., Dandona, R., Feigin, V., Freedman, G., Hubbell, B., Jobling, A., Kan, H., Knibbs, L., Liu, Y., Martin, R., Morawska, L., Pope, C.A., Shin, H., Straif, K., Shaddick, G., Thomas, M., van Dingenen, R., van Donkelaar, A., Vos, T., Murray, C.J.L., Forouzanfar, M.H., 2017. Estimates and 25-year trends of the global burden of disease attributable to ambient air pollution: an analysis of data from the Global Burden of Diseases Study 2015. Lancet 389, 1907–1918. https://doi.org/10.1016/S0140-6736(17)30505-6.

Dominici, F., McDermott, A., Zeger, S.L., Samet, J.M., 2002. On the use of generalized additive models in time-series studies of air pollution and health. Am. J. Epidemiol. 156, 193–203. https://doi.org/10.1093/aje/kwf062.

EU, 2016. Directive 2016/2284/EC of the European Parliament and of the Council of 14 December 2016 on the Reduction of National Emissions of Certain Atmospheric Pollutants, Amending Directive 2003/35/EC and Repealing Directive 2001/81/EC.

Fowler, D., Brunkreef, B., Fuzzi, S., Monks, P.S., Sutton, M.A., Brasseur, G.P., Friedrich, R., Passante, L.G., Jimenez-Mingo, J.M., 2013. Research Findings in Support of the EU Air Quality Review. Publications Office of the European Union, Luxembourg, p. 108 Available at. https://op.europa.eu/en/publication-detail/-/publication/2c4a737c-fc83-11e5-b713-01aa75ed71a1/language-en.

Garrido-Perez, J.M., Ordóñez, C., García-Herrera, R., Schnell, J.L., 2019. The differing impact of air stagnation on summer ozone across Europe. Atmos. Environ. 219, 117062. https://doi.org/10.1016/j.atmosenv.2019.117062.

Georgoulias, A.K., Van Der, R.A.J., Stammes, P., Folkert Boersma, K., Eskes, H.J., 2019. Trends and trend reversal detection in 2 decades of tropospheric NO_2 satellite observations. Atmos. Chem. Phys. 19, 6269–6294. https://doi.org/10.5194/acp-19-6269-2019.

Hersbach, H., Bell, B., Berrisford, P., Hirahara, S., Horányi, A., Muñoz-Sabater, J., Nicolas, J., Peubey, C., Radu, R., Schepers, D., Simmons, A., Soci, C., Abdalla, S., Abellan, X., Balsamo, G., Bechtold, P., Biavati, G., Bidlot, J., Bonavita, M., De Chiara, G., Dahlgren, P., Dee, D., Diamantakis, M., Dragani, R., Flemming, J., Forbes, R., Fuentes, M., Geer, A., Haimberger, L., Healy, S., Hogan, R.J., Hólm, E., Janisková, M., Keeley, S., Laloyaux, P., Lopez, P., Lupu, C., Radnoti, G., de Rosnay, P., Rozum, I., Vamborg, F., Villaume, S., Thépaut, J.N., 2020. The ERA5 global reanalysis. Q. J. R. Meteorol. Soc. https://doi.org/10.1002/qj.3803.

Hollaway, M., Wild, O., Yang, T., Sun, Y., Xu, W., Xie, C., Whalley, L., Slater, E., Heard, D., Liu, D., 2019. Photochemical impacts of haze pollution in an urban environment. Atmos. Chem. Phys. 19, 9699–9714. https://doi.org/10.5194/acp-19-9699-2019.

Ivanov, D., 2020. Predicting the impacts of epidemic outbreaks on global supply chains: a simulation-based analysis on the coronavirus outbreak (COVID-19/SARS-CoV-2) case. Transp. Res. Part E 136, 101922. https://doi.org/10.1016/j.tre.2020.101922.

Jacob, D.J., Winner, D.A., 2009. Effect of climate change on air quality. Atmos. Environ. 43, 51–63. https://doi.org/10.1016/j.atmosenv.2008.09.051.

Jhun, I., Coull, B.A., Zanobetti, A., Koutrakis, P., 2015. The impact of nitrogen oxides concentration decreases on ozone trends in the USA. Air Qual. Atmos. Health 8, 283–292. https://doi.org/10.1007/s11869-014-0279-2.

Jonson, J.E., Simpson, D., Fagerli, H., Solberg, S., 2006. Can we explain the trends in European ozone levels? Atmos. Chem. Phys. 6, 51–66. https://doi.org/10.5194/acp-6-51-2006.

Kalnay, E., Kanamitsu, M., Kistler, R., Collins, W., Deaven, D., Gandin, L., Iredell, M., Saha, S., White, G., Woollen, J., Zhu, Y., Chelliah, M., Ebisuzaki, W., Higgins, W., Janowiak, J., Mo, K.C., Ropelewski, C., Wang, J., Leetmaa, A., Reynolds, R., Jenne, R., Joseph, D., 1996. The NCEP NCAR 40-year reanalysis project. Bull. Am. Meteorol. Soc. 77, 437–472. https://doi.org/10.1175/1520-0477(1996)077<0437:TNYRP>2.0.CO;2.

Kleinman, L.I., Daum, P.H., Lee, Y.N., Nunnermacker, L.J., Springston, S.R., Weinstein-Lloyd, J., Rudolph, J., 2002. Ozone production efficiency in an urban area. J. Geophys. Res. Atmos. 107. https://doi.org/10.1029/2002JD002529.

Li, K., Jacob, D.J., Liao, H., Zhu, J., Shah, V., Shen, L., Bates, K.H., Zhang, Q., Zhai, S., 2019. A two-pollutant strategy for improving ozone and particulate air quality in China. Nat. Geosci. 12, 906–910. https://doi.org/10.1038/s41561-019-0464-x.

Lin, X., Trainer, M., Liu, S.C., 1988. On the nonlinearity of the tropospheric ozone production. J. Geophys. Res. 93, 879–888. https://doi.org/10.1029/jd093id12p15879.

Menut, L., Bessagnet, B., Siour, G., Mailler, S., Pennel, R., Cholakian, A., 2020. Impact of lockdown measures to combat Covid-19 on air quality over western Europe. Sci. Total Environ. 741, 140426. https://doi.org/10.1016/j.scitotenv.2020.140426.

Mills, G., Hayes, F., Simpson, D., Emberson, L., Norris, D., Harmens, H., Büker, P., 2011. Evidence of widespread effects of ozone on crops and (semi-)natural vegetation in Europe (1990–2006) in relation to AOT40- and flux-based risk maps. Glob. Chang. Biol. 17, 592–613. https://doi.org/10.1111/j.1365-2486.2010.02217.x.

Monks, P.S., Archibald, A.T., Colette, A., Cooper, O., Coyle, M., Derwent, R., Fowler, D., Granier, C., Law, K.S., Mills, G.E., Stevenson, D.S., Tarasova, O., Thouret, V., Von Schneidemesser, E., Sommariva, R., Wild, O., Williams, M.L., 2015. Tropospheric ozone and its precursors from the urban to the global scale from air quality to short-lived climate forcer. Atmos. Chem. Phys. 15, 8889–8973. https://doi.org/10.5194/acp-15-8889-2015.

Nicola, M., Alsafi, Z., Sohrabi, C., Kerwan, A., Al-Jabir, A., Iosifidis, C., Agha, M., Agha, R., 2020. The socio-economic implications of the coronavirus and COVID-19 pandemic: a review. Int. J. Surg. Open. 78, 185–193. https://doi.org/10.1016/j.ijsu.2020.04.018.

Ordóñez, C., Mathis, H., Furger, M., Henne, S., Hüglin, C., Staehelin, J., Prévôt, A.S.H., 2005. Changes of daily surface ozone maxima in Switzerland in all seasons from 1992 to 2002 and discussion of summer 2003. Atmos. Chem. Phys. 5, 1187–1203. https://doi.org/10.5194/acp-5-1187-2005.

Otero, N., Sillmann, J., Schnell, J.L., Rust, H.W., Butler, T., 2016. Synoptic and meteorological drivers of extreme ozone concentrations over Europe. Environ. Res. Lett. 11, 024005. https://doi.org/10.1088/1748-9326/11/2/024005.

Paoletti, E., De Marco, A., Beddows, D.C.S., Harrison, R.M., Manning, W.J., 2014. Ozone levels in European and USA cities are increasing more than at rural sites, while peak values are decreasing. Environ. Pollut. 192, 295–299. https://doi.org/10.1016/j.envpol.2014.04.040.

Parrish, D.D., Ryerson, T.B., Holloway, J.S., Trainer, M., Fehsenfeld, F.C., 1999. New directions: does pollution increase or decrease tropospheric ozone in winter-spring? Atmos. Environ. 33, 5147–5149. https://doi.org/10.1016/S1352-2310(99)00253-8.

Pearce, J.L., Beringer, J., Nicholls, N., Hyndman, R.J., Tapper, N.J., 2011. Quantifying the influence of local meteorology on air quality using generalized additive models. Atmos. Environ. 45, 1328–1336. https://doi.org/10.1016/j.atmosenv.2010.11.051.

Petetin, H., Bowdalo, D., Soret, A., Guevara, M., Jorba, O., Serradell, K., García-Pando, C.P., 2020. Meteorology-normalized impact of COVID-19 lockdown upon NO_2 pollution in Spain. Atmos. Chem. Phys. Discuss. https://doi.org/10.5194/acp-2020-446.

Saiz-Lopez, A., Borge, R., Notario, A., Adame, J.A., Paz, D.D. La, Querol, X., Artíñano, B., Gómez-Moreno, F.J., Cuevas, C.A., 2017. Unexpected increase in the oxidation capacity of the urban atmosphere of Madrid, Spain. Sci. Rep. 7, 1–11. https://doi.org/10.1038/srep45956.

Schnell, J.L., Prather, M.J., 2017. Co-occurrence of extremes in surface ozone, particulate matter, and temperature over eastern North America. Proc. Natl. Acad. Sci. 114, 2854–2859. https://doi.org/10.1073/pnas.1614453114.

Servén, D., Brummitt, C., 2018. pyGAM: generalized additive models in Python. Zenodo https://doi.org/10.5281/zenodo.1208723.

Shi, X., Brasseur, G.P., 2020. The response in air quality to the reduction of Chinese economic activities during the COVID-19 outbreak. Geophys. Res. Lett. 47, 1–8. https://doi.org/10.1029/2020GL088070.

Sicard, P., De Marco, A., Troussier, F., Renou, C., Vas, N., Paoletti, E., 2013. Decrease in surface ozone concentrations at Mediterranean remote sites and increase in the cities. Atmos. Environ. 79, 705–715. https://doi.org/10.1016/j.atmosenv.2013.07.042.

Sicard, P., De Marco, A., Agathokleous, E., Feng, Z., Xu, X., Paoletti, E., Rodriguez, J.J.D., Calatayud, V., 2020. Amplified ozone pollution in cities during the COVID-19 lockdown. Sci. Total Environ. 735, 139542. https://doi.org/10.1016/j.scitotenv.2020.139542.

Siciliano, B., Dantas, G., da Silva, C.M., Arbilla, G., 2020. Increased ozone levels during the COVID-19 lockdown: analysis for the city of Rio de Janeiro, Brazil. Sci. Total Environ. 737, 139765. https://doi.org/10.1016/j.scitotenv.2020.139765.

Sillman, S., 1999. The relation between ozone, NO_x and hydrocarbons in urban and polluted rural environments. Atmos. Environ. 33, 1821–1845. https://doi.org/10.1016/S1352-2310(98)00345-8.

Sohrabi, C., Alsafi, Z., O'Neill, N., Khan, M., Kerwan, A., Al-Jabir, A., Iosifidis, C., Agha, R., 2020. World Health Organization declares global emergency: a review of the 2019 novel coronavirus (COVID-19). Int. J. Surg. 76, 71–76. https://doi.org/10.1016/j.ijsu.2020.02.034.

Sun, W., Hess, P., Liu, C., 2017. The impact of meteorological persistence on the distribution and extremes of ozone. Geophys. Res. Lett. 44, 1545–1553. https://doi.org/10.1002/2016GL071731.

Thielmann, A., Prévôt, A.S.H., Grüebler, F.C., Staehelin, J., 2001. Empirical ozone isopleths as a tool to identify ozone production regimes. Geophys. Res. Lett. 28, 2369–2372. https://doi.org/10.1029/2000GL012787.

Tobías, A., Carnerero, C., Reche, C., Massagué, J., Via, M., Minguillón, M.C., Alastuey, A., Querol, X., 2020. Changes in air quality during the lockdown in Barcelona (Spain) one month into the SARS-CoV-2 epidemic. Sci. Total Environ. 726, 138540. https://doi.org/10.1016/j.scitotenv.2020.138540.

Tonse, S.R., Brown, N.J., Harley, R.A., Jin, L., 2008. A process-analysis based study of the ozone weekend effect. Atmos. Environ. 42, 7728–7736. https://doi.org/10.1016/j.atmosenv.2008.05.061.

Trainer, M., Parrish, D.D., Norton, R.B., Fehsenfeld, F.C., Anlauf, K.G., Bottenheim, J.W., Tang, Y.Z., Wiebe, H.A., Roberts, J.M., Tanner, R.L., Newman, L., Bowersox, V.C., Meagher, J.F., Olszyna, K.J., Rodgers, M.O., Wang, T., Berresheim, H., Demerjian, K.L., Roychowdhury, U.K., 1993. Correlation of ozone with NO_y in photochemically aged air. J. Geophys. Res. 98, 2917–2925. https://doi.org/10.1029/92JD01910.

Unger, N., Shindell, D.T., Koch, D.M., Amann, M., Cofala, J., Streets, D.G., 2006. Influences of man-made emissions and climate changes on tropospheric ozone, methane, and sulfate at 2030 from a broad range of possible futures. J. Geophys. Res. 111, D12313. https://doi.org/10.1029/2005JD006518.

Vogel, B., Riemer, N., Vogel, H., Fiedler, F., 1999. Findings on NO_y, as an indicator for ozone sensitivity based on different numerical simulations. J. Geophys. Res. Atmos. 104, 3605–3620. https://doi.org/10.1029/1998JD100075.

Waked, A., Sauvage, S., Borbon, A., Gauduin, J., Pallares, C., Vagnot, M.P., Léonardis, T., Locoge, N., 2016. Multi-year levels and trends of non-methane hydrocarbon concentrations observed in ambient air in France. Atmos. Environ. 141, 263–275. https://doi.org/10.1016/j.atmosenv.2016.06.059.

Wang, Y., Hao, J., McElroy, M.B., Munger, J.W., Ma, H., Chen, D., Nielsen, C.P., 2009. Ozone air quality during the 2008 Beijing Olympics: effectiveness of emission restrictions. Atmos. Chem. Phys. 9, 5237–5251. https://doi.org/10.5194/acp-9-5237-2009.

Wang, Y., Yuan, Y., Wang, Q., Liu, C., Zhi, Q., Cao, J., 2020. Changes in air quality related to the control of coronavirus in China: implications for traffic and industrial emissions. Sci. Total Environ. 731, 139133. https://doi.org/10.1016/j.scitotenv.2020.139133.

Witte, J.C., Schoeberl, M.R., Douglass, A.R., Gleason, J.F., Krotkov, N.A., Gille, J.C., Pickering, K.E., Livesey, N., 2009. Satellite observations of changes in air quality during the 2008 Beijing Olympics and Paralympics. Geophys. Res. Lett. 36, 1–6. https://doi.org/10.1029/2009GL039236.

Worden, H.M., Deeter, M.N., Frankenberg, C., George, M., Nichitiu, F., Worden, J., Aben, I., Bowman, K.W., Clerbaux, C., Coheur, P.F., De Laat, A.T.J., Detweiler, R., Drummond, J.R., Edwards, D.P., Gille, J.C., Hurtmans, D., Luo, M., Martínez-Alonso, S., Massie, S., Pfister, G., Warner, J.X., 2013. Decadal record of satellite carbon monoxide observations. Atmos. Chem. Phys. 13, 837–850. https://doi.org/10.5194/acp-13-837-2013.

Yan, Y., Pozzer, A., Ojha, N., Lin, J., Lelieveld, J., 2018. Analysis of European ozone trends in the period 1995–2014. Atmos. Chem. Phys. 18, 5589–5605. https://doi.org/10.5194/acp-18-5589-2018.

Yang, Y., Zhang, H., Chen, X., 2020. Coronavirus pandemic and tourism: dynamic stochastic general equilibrium modeling of infectious disease outbreak. Ann. Tour. Res. 102913. https://doi.org/10.1016/j.annals.2020.102913.